

MetamatBench: Integrating Heterogeneous Data, Computational Tools, and Visual Interface for Metamaterial Discovery

Jianpeng Chen
Virginia Tech
Blacksburg, Virginia, USA
jianpengc@vt.edu

Wangzhi Zhan
Virginia Tech
Blacksburg, Virginia, USA
wzhan24@vt.edu

Haohui Wang
Virginia Tech
Blacksburg, Virginia, USA
haohuiw@vt.edu

Zian Jia
Princeton University
Princeton, New Jersey, USA
University of Pennsylvania
Philadelphia, Pennsylvania, USA
zj1283@princeton.edu

Jingru Gan
University of California, Los Angeles
Los Angeles, California, USA
jrgan@cs.ucla.edu

Junkai Zhang
University of California, Los Angeles
Los Angeles, California, USA
jkzhang@g.ucla.edu

Jingyuan Qi
Virginia Tech
Blacksburg, Virginia, USA
jingyq1@vt.edu

Tingwei Chen
University of Tennessee, Knoxville
Knoxville, Tennessee, USA
cccchentingwei@gmail.com

Lifu Huang
University of California, Davis
Davis, California, USA
lfuhuang@ucdavis.edu

Muhao Chen
University of California, Davis
Davis, California, USA
muhchen@ucdavis.edu

Ling Li
University of Pennsylvania
Philadelphia, Pennsylvania, USA
lzli@seas.upenn.edu

Wei Wang
University of California, Los Angeles
Los Angeles, California, USA
weiwang@cs.ucla.edu

Dawei Zhou
Virginia Tech
Blacksburg, Virginia, USA
zhoud@vt.edu

Abstract

Metamaterials, engineered materials with architected structures across multiple length scales, offer unprecedented and tunable mechanical properties that surpass those of conventional materials. However, leveraging advanced machine learning (ML) for metamaterial discovery is hindered by three fundamental challenges: (C1) Data Heterogeneity Challenge arises from heterogeneous data sources, heterogeneous composition scales, and heterogeneous structure categories; (C2) Model Complexity Challenge stems from the intricate geometric constraints of ML models, which complicate their adaptation to metamaterial structures; and (C3) Human-AI Collaboration Challenge comes from the “dual black-box” nature of sophisticated ML models and the need for intuitive user interfaces. To tackle these challenges, we introduce a unified framework, named MetamatBench, that operates on three levels. (1) At the *data level*, we integrate and standardize 5 heterogeneous, multi-modal metamaterial datasets. (2) The *ML level* provides a comprehensive toolkit that adapts 17 state-of-the-art ML methods for metamaterial discovery. It also includes a comprehensive evaluation suite with 12 novel performance metrics plus a finite element-based assessment to ensure accurate and reliable model validation. (3) The *user level* features

a visual-interactive interface that bridges the gap between complex ML techniques and non-ML researchers, advancing property prediction and inverse design of metamaterials for research and applications. MetamatBench offers a unified platform that enables ML researchers and practitioners to develop and evaluate new methodologies in metamaterial discovery. For accessibility and reproducibility, we open-source our benchmark and the codebase at <https://github.com/cjpcool/Metamaterial-Benchmark>.

CCS Concepts

• **Information systems** → **Database design and models**; • **Human-centered computing** → *Systems and tools for interaction design*; • **Applied computing** → *Engineering*.

Keywords

Metamaterial Discovery, Benchmark, AI for Science.

ACM Reference Format:

Jianpeng Chen, Wangzhi Zhan, Haohui Wang, Zian Jia, Jingru Gan, Junkai Zhang, Jingyuan Qi, Tingwei Chen, Lifu Huang, Muhao Chen, Ling Li, Wei Wang, and Dawei Zhou. 2025. MetamatBench: Integrating Heterogeneous Data, Computational Tools, and Visual Interface for Metamaterial Discovery. In *Proceedings of the 31st ACM SIGKDD Conference on Knowledge Discovery and Data Mining V.2 (KDD '25)*, August 3–7, 2025, Toronto, ON, Canada. ACM, New York, NY, USA, 15 pages. <https://doi.org/10.1145/3711896.3737416>



This work is licensed under a Creative Commons Attribution 4.0 International License. *KDD '25, Toronto, ON, Canada*

© 2025 Copyright held by the owner/author(s).
ACM ISBN 979-8-4007-1454-2/2025/08
<https://doi.org/10.1145/3711896.3737416>

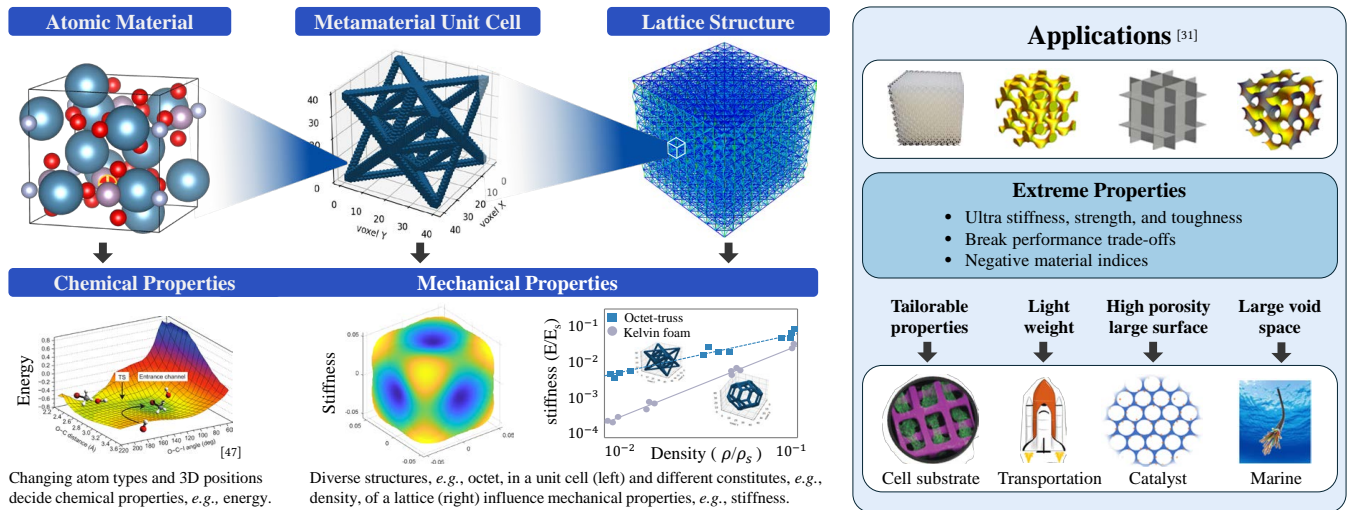


Figure 1: An overview of metamaterials. Metamaterials are microstructured materials with effective material properties beyond their compositions. The multiscale architecture of metamaterial enables high mechanical efficiency and unusual properties, showing great potential in applications like biomedical devices, transportation systems, robotics, etc.

1 Introduction

Metamaterials are an emerging class of materials that achieve unusual material properties through designed architecture at multiple length scales. They have been extensively studied in the past decades for their superior, tunable, and programmable material properties, demonstrating huge potential in diverse applications [22, 50]. As illustrated in Figure 1 (left), while conventional material properties are dominated by their atomic structure [47, 66], architected metamaterials emphasize the structure of a material, with scales ranging from the nano- and micro-scales up to macro-scale. Therefore, studies on metamaterials, *e.g.*, truss-based metamaterials, often focus on designing the geometric structure of a unit cell. Micro-lattice materials have shown high stiffness, damage tolerance, reconfigurable and programmable properties, and even negative material indices (such as negative Poisson’s ratio and negative thermal conductivity) [31]. Such high performance with unusual properties drives the wide application of metamaterials in various engineering fields (lightweight metamaterial empowers space transport systems, large void space metamaterials enhance marine application, low thermal conductivity metamaterials are applied to thermal protection systems, *etc.*), as shown in Figure 1 (right).

Because of their truss-based geometric characteristics, metamaterials are typically modeled as 3D graphs composed of nodes and edges to study how their 3D structures influence mechanical properties. Existing works [3, 26, 46, 68] generally employ graph neural networks (GNNs) [17, 35, 36] to capture the structural information for mechanical property prediction [29, 46] or metamaterial inverse design [42, 52, 68]. In parallel, advanced studies in geometric machine learning (ML) have extensively explored techniques to integrate rich 3D structural information in molecules [6, 10, 18, 23, 25, 38, 41, 56, 58, 61] and crystal researches [32, 44, 62, 63, 67]. Although many studies have benchmarked these methods on atomic crystal and molecular scales [7, 20, 21, 40], it remains unclear how advanced geometric ML approaches perform in the multiscale metamaterial

domain. Consequently, there is a critical need to establish a standardized benchmark and evaluation platform that bridges the gap between current metamaterial modeling techniques and advanced geometric ML approaches, ensuring comprehensive integration and assessment of 3D structural information in metamaterial discovery.

In this paper, we identify three key challenges in constructing a metamaterial benchmark. **C1: Data heterogeneity.** This challenge arises from (1) diverse data sources, *e.g.*, structural geometry, mechanical properties, and experimental measurements, (2) complex structure categories, *e.g.*, trusses, shells, foams, *etc.*, and (3) rich properties *e.g.*, stiffness and modulus. **C2: Model complexity.** The second challenge stems from the complexity of ML models and their potential incompatibility with multiscale metamaterials. Specifically, these ML models typically have a complex taxonomy with various backbones and geometric constraints. Additionally, they generally target atomic graphs and chemical properties, which are typically incompatible with metamaterials. These complexities pose challenges to evaluating and benchmarking advanced ML models on metamaterial applications. How to integrate and evaluate these complex ML models is a problem of pressing needs. **C3: Human-AI collaboration.** A goal of this work is to empower metamaterial researchers to easily leverage advanced ML models to accelerate progress in related fields. Achieving this requires fostering effective human-AI collaboration across diverse research domains. On one hand, sophisticated ML models often function as black box for researchers who may lack expert knowledge about advanced ML models. Instead, a visual-interactive interface may help researchers interact with the AI system. On the other hand, human users are also black box for the AI system. It is hard for the AI system to anticipate how researchers use it. To address this “dual black-box” challenge, a *human-AI collaborative* interface is essential to facilitate metamaterial research.

In this paper, we propose MetamatBench as shown in Figure 3, which contributes to the data level, ML level, and user level, establishing a robust, comprehensive, and user-friendly benchmark system. Within MetamatBench, the data level combines heterogeneous and multi-modal data sources into a unified framework to tackle the first challenge. The intermediate ML level consists of a model toolbox and an evaluation toolbox. The model toolbox focuses on two fundamental tasks, and assembles a wide range of ML models with various geometric characteristics for a comprehensive comparison. The evaluation toolbox employs a multi-perspective evaluation framework with several novel metrics to ensure robust evaluations. The topmost user level emphasizes human-AI collaboration, mitigating the dual black-box issue by providing a visual-interactive interface. This three-level system is integrated to advance the exploration and research of metamaterials. To the best of our knowledge, MetamatBench is the first benchmark for metamaterial that integrates heterogeneous data, ML models, novel metrics, and a visual-interactive interface. The overall contributions can be summarized as follows.

- **Database Development:** We collect and process five metamaterial datasets covering multi-modal lattice structures, and unify the representation of three 3D graph metamaterial datasets.
- **ML Toolbox Development:** We introduce a *model toolbox* that integrates 17 models designed for 3D crystal materials and molecules, and adapts them to metamaterial learning to assess their effectiveness in metamaterial tasks. Moreover, we develop a *evaluation toolbox* that includes an evaluation framework with novel metrics for robust metamaterial assessment and finite element (FE) computation-based metrics for physics-aware evaluation.
- **Visual-Interactive Interface Development:** We design a visual-interactive interface to facilitate human-AI collaboration and data visualization. This interface helps metamaterial researchers explore advanced methods and choose appropriate ML models, thereby bridging the gap between metamaterial research and ML. We publish the code for the visual-interactive interface that allows for local deployment.
- **Open-Sourced Codebase:** For accessibility and reproducibility, we have open-sourced our benchmark and the codebase at <https://github.com/cjpcool/Metamaterial-Benchmark>.

2 Preliminary

2.1 Previous Benchmarks

In recent years, many benchmarks of ML for scientific discovery have emerged with the breakthroughs made in AI for science [33, 60, 67]. These benchmarks have explored the application of complex ML to 3D atomic-scale scientific discovery. However, they generally focus on crystal or molecular materials with chemical properties, as demonstrated in the top part of Table 1. For instance, [13, 14, 16, 21, 30, 51, 55] focus on benchmarking crystal materials where atom type and chemical properties dominate the learning space, and [12, 53] benchmark ML models on molecular space that is also based on atom type and chemical properties. The metamaterials that specifically focus on multiscale architectures and mechanical properties still lack exploration. Therefore, to fill the gap, a comprehensive metamaterial benchmark with a unified representation is needed.

2.2 Unified Metamaterial Representation

To address data heterogeneity (C1), we introduce a metamaterial representation to unify 3D graph datasets and benchmark them with advanced geometric graph learning methods. This unified metamaterial representation considers a six-dimensional learning space, de-emphasizing atomic element information while highlighting structural lattice characteristics. In general, we denote $\mathcal{M}(\mathbf{L}, \mathcal{U}, \mathbf{y})$ as a metamaterial. Figure 2 illustrates the hierarchical six-dimensional learning space of a metamaterial considering the necessary details of *unit cell* and *lattice* for *metamaterial* applications. The six dimensions of the learning space are labeled D1 through D6 for reference:

Definition 1 (Metamaterial Property). *The mechanical properties of a metamaterial (D1) are represented as $\mathbf{y} \in \mathbb{R}^d$, where d is the property dimension.*

Definition 2 (Lattice Representation). *The metamaterial lattice structure (D2) is denoted by $\mathbf{L} = [\mathbf{l}_0, \mathbf{l}_1, \mathbf{l}_2]^T \in \mathbb{R}^{3 \times 3}$, where $\mathbf{l}_d \in \mathbb{R}^3$, capturing the periodic angles and lattice lengths in 3D space.*

Definition 3 (Unit Cell Representation). *The metamaterial unit cell is represented by $\mathcal{U}(\mathbf{P}, \mathbf{X}, \mathbf{E}, \mathbf{D})$, composed of four components: node coordinates (D3), node attributes (D4), edge connections (D5), and Edge attributes (D6).*

To be specific, **node coordinates (D3)** denote the N node positions in 3D Cartesian system: $\mathbf{P} = [\mathbf{p}_0, \mathbf{p}_1, \dots, \mathbf{p}_{N-1}]^T \in \mathbb{R}^{N \times 3}$, where $\mathbf{p}_i \in \mathbb{R}^3$. In addition, we provide the transformed fractional coordinates in the unified representation for convenient computation. **Node attributes (D4)** $\mathbf{X} \in \mathbb{R}^{N \times 4}$ denotes the specifically designed one-hot encoding of four types of N nodes, *i.e.*, face node, corner node, edge node, and inner node, as depicted in Figure 2. Unlike atomic graphs, where node attributes naturally depict the element type, the designed representation of node attributes emphasizes structural information. Specifically, similar to [26], we classify all nodes into outer nodes and inner nodes, where inner nodes are the nodes inside the unit cell while outer nodes are shared by multiple unit cells in a lattice since the periodical repetition, for example, face nodes are shared by two unit cells, edge nodes are shared by four unit cells, and corner nodes are shared by eight unit cells.

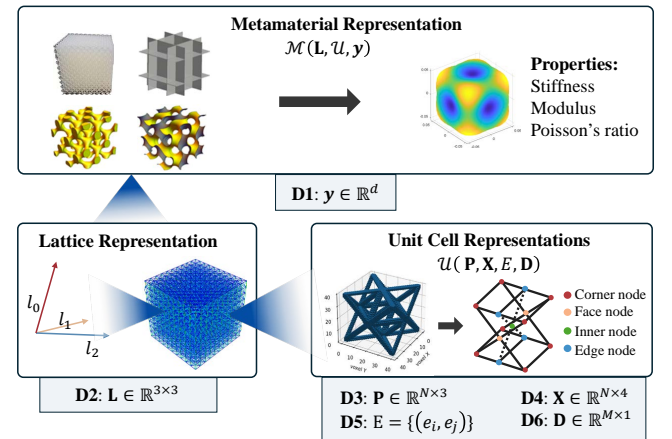


Figure 2: Unified metamaterial representation.

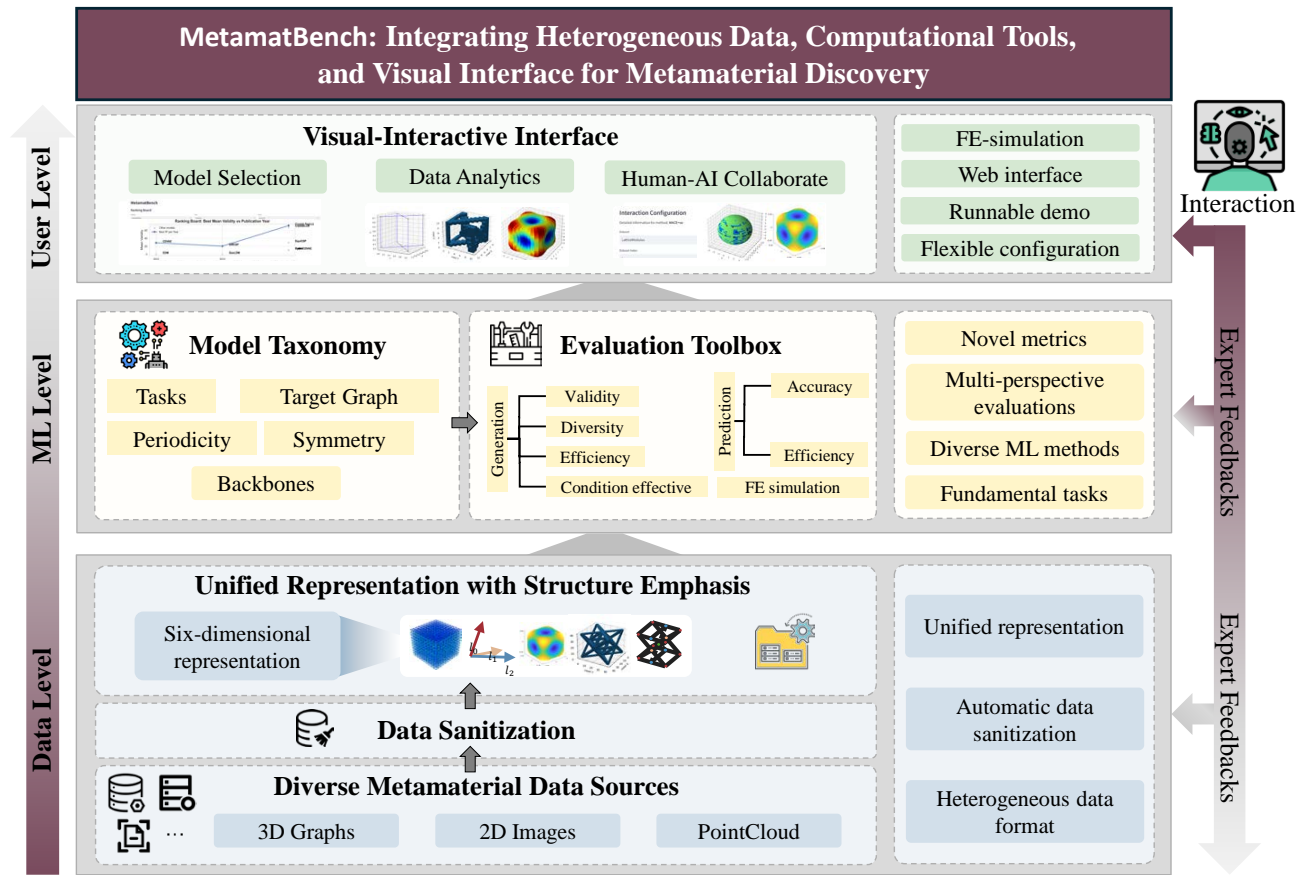


Figure 3: An overview of MetamatBench: bottom dataset level provides a base for various metamaterial applications; middle ML level includes ML models and evaluation toolbox benefits researchers in finding the best suitable models; top user level visual-interactive interface enables human-AI dual black-box collaborations.

Edge connections (D5) $E = \{(e_i, e_j)\}$ describe the edges between i -th and j -th node. **Edge attributes (D6)** $D \in \mathbb{R}^{M \times 1}$ record the auxiliaries for M edges, e.g., edge diameter which determines the density of a unit cell.

3 MetamatBench Development

3.1 MetamatBench: Overview

MetamatBench is a multi-level system containing data level, ML level, and user level, as illustrated in Figure 3. In this section, we introduce the development of MetamatBench from bottom to top, i.e., from database development (Section 3.2), ML model toolbox and evaluation toolbox development (Section 3.3), to visual-interactive interface development (Section 3.4).

3.2 MetamatBench: Database Development

The data level aims to mitigate data heterogeneity challenges (C1) by collecting and preprocessing various data sources to a unified data representation. Overall, Table 1 compares the datasets included in MetamatBench (bottom portion of the table) to those commonly

used in prior work (top portion). It shows that MetamatBench includes a large number of datasets with a specific focus on metamaterial and mechanical properties. MetamatBench collects heterogeneous metamaterial datasets across multiple modalities. We then apply a unified data sanitization process and use the unified metamaterial representation (defined in Section 2.2) for the integrated 3D graph datasets. This unified process enables fair evaluation of different 3D graph models, and it also paves the way for future exploration with multiple data modalities for metamaterial design.

Heterogeneous Data Sources. Metamaterials often require complicated structures to achieve desired properties, which can be difficult to design and predict. Therefore, we anticipate that the integration of multi-modal data will alleviate this challenge and further advance the field, attracting more researchers to explore this topic. We collect three modalities of datasets in this benchmark, including three 3D graph-based datasets (MetaStiffness [9], MetaModulus [42], and MetaTruss [68]), one 2D image dataset (LagrangianFrame [8]), and one point cloud dataset (PointCloud [15]). To be specific, *MetaModulus* [42] is a metamaterial dataset constructed from two publicly accessible crystal material databases,

RCSR [49] and EPICNET [54]. This dataset provides three properties, *i.e.*, Young’s modulus, Shear modulus, and Poisson’s ratio. *MetaStiffness* [9] is a dataset that employs seven fundamental lattices to construct metamaterials. By combining three lattice types, 262 unique topologies are generated, with additional variants produced through rotation and scaling transformations. Each structure’s stiffness tensor is characterized by 21 independent elastic constants. *MetaTruss* [68] is generated from five elementary truss lattices, randomly adding or deleting edges and adjusting the node positions. It filters out the physically invalid lattices and randomly selects lattices to construct the final dataset. *LagrangianFrame* [8] proposes representing metamaterials in a Lagrangian frame (instead of the traditional Eulerian frame) and provides a 2D dataset of metamaterial structures generated in this Lagrangian coordinate system. *PointCloud* [15] produces 29,400 3D point-cloud data constructed by sampling existing datasets to avoid inherent data biases.

Data Sanitization. We observe several issues (described below) on these datasets, leading to the collected datasets not being directly applicable for benchmarking. Therefore, we design a multi-perspective prototype following previous works [9, 68] to filter out invalid structures for these datasets. This prototype includes following hard constraints to automatically filter out invalid structures, and it is also considered in our proposed evaluation toolbox for validity evaluation.

- **Metamaterial-Oriented Sanitization:** At the metamaterial level, we observe that some property values are missing in the datasets. For example, many lattices in MetaModulus dataset miss the property of Poisson’s ratio. Therefore, these samples with missing values are filtered out to ensure data completeness.
- **Lattice-Oriented Sanitization:** At the lattice level, we discover that the node coordinates might exceed the lattice range, *e.g.*, some nodes in MetaModulus. In addition, we find that some nodes in MetaModulus dataset are extremely close. Therefore, we propose *distance restriction* to filter out these lattices with dispersed or clustered nodes. The lattices containing node distances larger than lattice lengths or smaller than a specified threshold are identified and subsequently removed from the dataset.
- **Unit-Cell-Oriented Sanitization:** At the unit cell level, we find that some structures are invalid. For instance, many unit cells in MetaModulus are physically invalid. We propose that the unit cell (node connection patterns) of metamaterials should satisfy:
 - (1) *Connection graph*: all structures should be connected graphs.
 - (2) *Dangling restriction*: there are no dangling nodes in a structure, *i.e.*, all nodes have at least two edges connecting to other nodes.

After conducting these hard constraints for sanitization, the heterogeneity of three collected datasets is reduced (as analyzed in Section 4.1). The final data statistics are summarized in the bottom rows of Table 1. More statistics can be found in Appendix E.1.

3.3 MetamatBench: ML Toolbox Development

The ML level development aims to integrate and evaluate advanced ML levels for metamaterials applications by addressing the model complexity challenge (C2). In the ML toolbox, we assemble 17 state-of-the-art ML models (Table 2) into a model toolbox and propose a comprehensive evaluation toolbox with 12 novel metrics (Table 3) to evaluate ML models’ effectiveness on metamaterial applications.

Model Toolbox. Our model toolbox focuses on two fundamental tasks (*i.e.*, metamaterial generation and property prediction) and assembles a wide range of ML models with various geometric characteristics for a comprehensive comparison. Specifically, to compare 3D graph models for metamaterials, we consider both emerging 3D crystal graph models and the well-developed 3D molecule graph models. These two research areas focus on different aspects of 3D graphs while still sharing similarities for benchmarking metamaterial-based tasks. For example, crystal-targeted models should preserve periodic symmetries due to the periodic nature of the material [45], which is not necessary for molecules. Instead, the latter requires completeness for distinguishing molecule chirality [34, 57]. In addition, we specifically compare the performance of two mainstream types of 3D graph models, *i.e.*, equivariant and invariant models [11], on metamaterial datasets.

Overall, to benchmark 3D graph models on metamaterial, the proposed taxonomy in Figure 3 covers: (1) generative models and predictive models, (2) crystal material, molecular, and metamaterial graph models, (3) models with different periodicity constraints, (4) models with symmetry constraints, such as equivariant model and invariant model, and (5) models with various backbones. The detailed model taxonomy is summarized in Table 2.

Based on this taxonomy, we benchmark the two fundamental tasks, *i.e.*, prediction task and generation task. Both tasks are crucial in measuring the effectiveness of ML models for metamaterial learning in various application scenarios.

Evaluation Toolbox. We develop a novel evaluation framework in the ML toolbox to evaluate ML models for metamaterial applications. Adopting a multi-perspective approach, our evaluation framework is designed to provide robust and unbiased assessments of metamaterial models. This is accomplished by incorporating and adapting established metrics from previous works [9, 42, 44, 62, 68] and by developing new metrics that capture the unique characteristics of metamaterials. As illustrated in Table 3, property prediction task focuses on accuracy through a combination of three metrics, while generation task evaluates model performance based on the validity, diversity, and conditional effectiveness of the generated lattices. Additionally, the overall evaluation also considers the efficiency of both training and testing processes. More details of the evaluation toolbox are illustrated in Appendix C. Here, we provide several definitions for unbiased generative evaluation metrics. First, we define a symmetric node as a node that can find its central symmetric counterpart within an error range:

Definition 4 (Symmetric Node). *Consider node i with coordinates \mathbf{p}_i , the node is a symmetric node if there exists another node j in the structure that satisfies: $\|\mathbf{p}_i + \mathbf{p}_j - 2\mathbf{p}_c\|_2 < \epsilon$, where \mathbf{p}_c denotes central coordinates in the structure, and ϵ is a positive hyperparameter.*

In addition, the symmetry degree of a node is defined as the error value of the corresponding "most symmetric" node pair divided by the distance between the central coordinates and the farthest node.

Definition 5 (Symmetry Degree). *The symmetry degree of node i in a structure is defined as: $s_{degree_i} = \frac{\epsilon_{max} - s_{error_i}}{\epsilon_{max}}$, where $\epsilon_{max} = \max_j \|\mathbf{p}_c - \mathbf{p}_j\|_2$, $s_{error_i} = \min_j \|\mathbf{p}_i + \mathbf{p}_j - 2\mathbf{p}_c\|_2$, \mathbf{p}_c denotes central coordinates in this structure, and j is a node in this structure.*

Table 1: Comparison of material datasets. The upper group includes conventional atomic-scale materials commonly used in ML. The lower five datasets, collected by MetamatBench, focus on metamaterials with specialized mechanical properties.

Dataset	Design Target	Periodic	Property	# Samples
Carbon24 [51]	Atomic-scale crystalline materials	✓	Energy	10,153
Perov5 [13, 14]	Perovskite-type crystalline materials	✓	Energy	18,928
MP20 [30]	Crystalline atomic materials	✓	Chemical properties	45,231
MatBench [21]	Inorganic bulk materials	✓	Chemical properties	312–132,752
OC20 [16]	Bulk-adsorbate interface materials	✗	Energetic	640,081
QMOF [55]	Metal–organic framework (MOF) materials	✓	Chemical properties	>20,000
QM9 [53]	Molecular compounds	✗	Chemical properties	~134,000
OMDB [12]	Organic crystalline materials	✓	Electronics	12,500
MetaModulus [42]	Architected truss metamaterials for modulus design	✓	Three mechanical properties	16,707
MetaStiffness [9]	Architected truss metamaterials for stiffness optimization	✓	Elastic constants	1,048,575
MetaTruss [68]	Architected truss metamaterials for homogeneous stiffness	✓	Homogeneous stiffness	965,736
PointCloud [15]	Truss metamaterials (3D point-cloud representation)	✓	Mechanical properties	29,400
LagrangianFrame [8]	Shell and truss metamaterials (2D Lagrangian frame)	✓	Stress and strain	53,007

Table 2: The statistics of comparison methods. * indicates conditional generation support. Abbreviations: Trans Inv. (Translation Invariance), Glob (Global), Equiv. (Equivariant), Rot. (Rotation), VAE (Variational Auto Encoder), Diff (Diffusion), MPNN (Message Passing Neural Networks), GCN (Graph Convolutional Networks), LatDiff (Latent Diffusion), Perm. (permutation).

Methods	Task	Design Target	Periodicity	Symmetry	Backbone
EDM* [28]	Generation	Molecule	N/A	Equiv.	Diff
GeoLDM* [65]	Generation	Molecule	N/A	Equiv.	LatDiff
DiffCSP [32]	Generation	Crystal	Trans Inv.	Equiv. (lacks lattice Perm. Equiv.)	Diff
CDVAE [62]	Generation	Crystal	Trans Inv.	Inv Enc + Equiv Dec	VAE+Diff
EquiCSP [39]	Generation	Crystal	Trans Inv. + Perm Eq.	Equiv.	Diff
Cond-CDVAE* [43]	Generation	Crystal	Trans Inv.	Inv Enc + Equiv Dec	VAE+Diff
SyMat [44]	Generation	Crystal	Trans Inv.	Inv Enc + Inv Dec	VAE+Diff
Crystal-Text-LLM* [27]	Generation	Crystal	N/A	N/A	GPT-2
CrystaLLM* [4]	Generation	Crystal	N/A	N/A	LLaMA-2
SchNet [58]	Prediction	Molecule	N/A	Glob Inv	MPNN
SphereNet [41]	Prediction	Molecule	N/A	Glob Inv	MPNN
Equiformer [37]	Prediction	Molecule	N/A	Equiv.	MPNN
ViSNet [61]	Prediction	Molecule	Trans. + Rot. Inv	Equiv.	MPNN
CGCNN [63]	Prediction	Crystal	Trans Inv.	Glob. Inv.	GCN
ALIGNN [19]	Prediction	Crystal	Trans Inv.	Glob Inv	GCN
UniTruss [69]	Prediction	Metamaterial	N/A	N/A	VAE
MACE+ve [26]	Prediction	Metamaterial	N/A	Equiv.	MPNN

We then introduce periodicity, denoted as \mathcal{V}_p , to assess the generated structures at the lattice level. This metric aims to evaluate whether the structures can repeat for constructing a lattice. Formally, we define the necessary condition of periodicity of a structure, e.g., if a lattice is periodically valid, it must satisfy this definition, as follows.

Definition 6 (Periodicity). *Given a structure with node positions \mathbf{P} and lattice vectors \mathbf{L} , for each dimension $d \in \{0, 1, 2\}$, there exist at least one pair of coordinate points \mathbf{p}_i and \mathbf{p}_j s.t. $\|(\mathbf{p}_i + \mathbf{l}_d) - \mathbf{p}_j\|_1 < \epsilon$, where $\|\cdot\|_1$ is the L1 norm and ϵ is the tolerance range.*

In addition to ML-level evaluation, we also include an FE simulation tool in this toolbox, which can accurately predict elastic properties given the lattice graphs. This simulation tool enables researchers to make more informed decisions.

In summary, we develop the evaluation toolbox from 5 perspectives (i.e., validity, diversity, conditional effectiveness, accuracy, and efficiency) with 12 metrics, plus an FE simulation tool for physics-aware computation.

3.4 MetamatBench: Visual-Interactive Interface Development

At the user level, MetamatBench provides a web interface to address the human-AI collaboration challenge (C3). The visual-interactive interface consists of three main modules as shown in Figure 4, i.e., Ranking Board (M1), Dataset Interaction (M2), and Model Interaction (M3), that mitigate human-AI dual black-box issue.

M1: Model Selection. The Model Selection module provides a ranking board for overview of the advanced ML models’ performance on metamaterials. Users can choose the datasets, tasks, and metrics they are interested in for visualization.

M2: Dataset Analytics. This module provides an interface for users to interact with data level, analyzing the intrinsic data distributions. Users can not only view overall dataset statistics but also visualize and simulate the metamaterials and their corresponding properties. This helps researchers identify the dataset they need.

Table 3: Overall framework of the proposed evaluation toolbox. N_L is the number of generated structures.

Task	Perspective	Metric
Generation	Validity	<ul style="list-style-type: none"> • Dangling Restriction (Node Level): $\mathcal{V}_{DR} = 1 - \frac{N_D}{N_L}$, where N_D is the number of structures that contain dangling node. • Connectivity (Edge Level): $\mathcal{V}_C = \frac{N_C}{N_L}$, where N_C is the number of structures that are connected graph. • Symmetry (Unit Cell Level): $\mathcal{V}_S = \frac{1}{N_L} \sum_{k=1}^{N_L} \frac{N_{S_k} \cdot \sum_{i=1}^{N_k} s_{degree_i}}{(N_k)^2}$, where N_k is the node number of k-th structure, and N_{S_k} is the number of Symmetrical Node that is defined in Definition. 4 in k-th structure, and s_{degree_i} denotes Symmetry Degree that is defined in Definition 5. • Periodicity (Lattice Level): $\mathcal{V}_P = \frac{N_P}{N_L}$, where N_P denotes the number of generated structures that satisfy Definition 6.
	Diversity	<ul style="list-style-type: none"> • Coverage Recall: $COV_R = \frac{1}{N_t} \{i \in [1, \dots, N_L] : \exists k \in [1, \dots, N_L], D(\mathbf{P}_i^*, \mathbf{P}_k) < \epsilon_{cov}\}$, where $D(\cdot)$ denotes structural distance. Given an error bar ϵ_{cov}, N_t test structures, and node positions \mathbf{P}_i and \mathbf{P}_j^* of i-th and j-th structures. • Coverage Precision: $COV_P = \frac{1}{N_t} \{i \in [1, \dots, N_L] : \exists k \in [1, \dots, N_L], D(\mathbf{P}_i, \mathbf{P}_k^*) < \epsilon_{cov}\}$.
	Conditional Effectiveness (Figure 7)	<p>Conditional effectiveness is the mean of all N_L distances: $\frac{1}{N_L} \sum_i^{N_L} \min_{j \in 1, \dots, K} \text{Dist}(\mathbf{y}_i, \mathbf{y}_{i,j})$, where Dist is euclidean distance. The $\{\mathbf{y}_i\}_{i=1}^{N_L}$ and $\{\mathbf{y}_i, j\}_{j=k}^K$ are obtained by four steps.</p> <p>Step 1: Generate N_L lattices conditioned on N_L properties $\{\mathbf{y}_i\}_i^{N_L}$.</p> <p>Step 2: For each generated lattice, find K-nearest neighbors in test dataset by KNN algorithm.</p> <p>Step 3: For each i-th generated lattice, Map K neighbors to property space, obtaining $\{\mathbf{y}_{i,k}\}_k^K$.</p> <p>Step 4: For each i-th condition and corresponding K properties $\{\mathbf{y}_k\}_k^K$, compute minimum euclidean distance.</p>
	Efficiency	<ul style="list-style-type: none"> • Mean Evaluation Time (MET): Mean generation time per sample. • Mean Training Time (MTT): Mean training time per batch.
Prediction	Accuracy	<ul style="list-style-type: none"> • $MAE = \frac{1}{n} \sum_{i=1}^n \ \mathbf{y}_i - \hat{\mathbf{y}}_i\ _1$, where \mathbf{y} and $\hat{\mathbf{y}}$ denote the predicted and ground truth properties. • $NRMSE = \frac{\sqrt{\frac{1}{n} \sum_{i=1}^n \ \mathbf{y}_i - \hat{\mathbf{y}}_i\ ^2}}{\max(\mathbf{y}) - \min(\mathbf{y})}$. • $R^2 = 1 - \frac{\sum_{i=1}^n \ \mathbf{y}_i - \hat{\mathbf{y}}_i\ ^2}{\sum_{i=1}^n \ \mathbf{y}_i - \bar{\mathbf{y}}\ ^2}$, where $\bar{\mathbf{y}}$ denotes the mean of the observed values.
	Efficiency	<ul style="list-style-type: none"> • Mean Evaluation Time (MET): Mean prediction time per batch. • Mean Training Time (MTT): Mean training time per batch.
FE Simulation	Stiffness Computation	Use high-fidelity Finite Element (FE) simulation for accurate mechanical properties calculations, incorporating simulation and visualization of asymptotic homogenization [1, 2, 5, 48] to evaluate physics consistency.

M3: Human-AI Collaboration. This module enables easy calls for the proposed toolbox at the ML level. Users can specify the ML model and the datasets they wish to use, specify samples or conditions, and make predictions or generate results. The outcomes are visualized and can be simulated through the interface. By visualizing results and allowing parameter tweaks, the interface helps demystify the dual black-box of AI-assisted metamaterial design.

Table 4: Data sanitization analysis.

Dataset	$\mathcal{V}_{DR}\%$	$\mathcal{V}_C\%$	$\mathcal{V}_S\%$	$\mathcal{V}_P\%$
Original	15.10	62.71	90.06	99.16
Processed	24.07	100.00	94.92	99.13

4 Results and Analysis

In this section, we conduct extensive experiments to evaluate the efficacy of the proposed framework MetamatBench at the data level, ML level, and user level.

4.1 Data Validity Analysis

Here, we aim to show the effectiveness of the proposed unified data sanitization, thus mitigating C1. Table 4 shows the dataset statistics before and after our sanitization process (using MetaModulus as an example). We applied the validity evaluation metrics regarding four levels, *i.e.*, dangling restrictions \mathcal{V}_{DR} , connectivity \mathcal{V}_C , symmetry \mathcal{V}_S and periodicity \mathcal{V}_P as in Table 3, to both the original and the sanitized versions of the dataset. We observe that the validation metrics (\mathcal{V}_{DR} , \mathcal{V}_C , and \mathcal{V}_S) have increased after data sanitization, and \mathcal{V}_P value maintains more than 99%. The results demonstrate the effectiveness of the unified sanitization process. More statistical details of the database are provided in Appendix E.1.

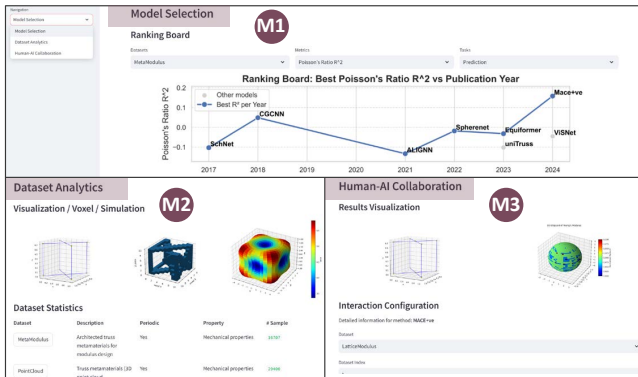
**Figure 4: Overview of the visual-interactive interface.**

Table 5: Generation Evaluation. DR: Dangling Restriction, Conn: Connectivity, Sym: Symmetry, Peri: Periodicity, CR: Coverage Recall, CP: Coverage Precision, MET: Mean Evaluation Time (generation time per sample), MTT: Mean Training Time.

Approach	Validity \uparrow					Diversity \uparrow			Cond. Effectiveness \downarrow	Efficiency	
	$\mathcal{V}_{DR}\%$	$\mathcal{V}_C\%$	$\mathcal{V}_S\%$	$\mathcal{V}_P\%$	Mean	Cov R.%	Cov P.%	Mean		MET (s)	MTT (ms)
Molecule targeted methods.											
EDM [28]	N/A	N/A	0.00	0.00	0.00	0.00	0.00	0.00	982.13	3.18	161.39
GeoLDM [65]	N/A	N/A	0.04	0.00	0.02	0.00	0.00	0.00	60.59	2.84	606.80
Crystal targeted methods.											
CDVAE [62]	N/A	N/A	57.03	0.40	28.72	55.85	95.80	75.83	N/A	93.00	97.42
DiffCSP [32]	N/A	N/A	34.46	6.50	20.48	95.80	96.65	96.23	N/A	2.97	63.79
EquiCSP [39]	N/A	N/A	55.37	3.55	29.46	100.00	52.35	76.18	N/A	1.90	64.57
Cond-CDVAE [43]	N/A	N/A	19.37	2.00	10.69	68.60	80.50	74.55	0.2050	225.01	314.51
SyMat [44]	N/A	N/A	41.10	0.00	20.55	79.34	38.90	59.12	N/A	89.49	141.20
CrystalLLM [4]	3.60	26.90	76.43	92.10	49.76	100.00	100.00	100.00	0.0983	2.08	14.51s
Crystal-Text-LLM [27]	23.50	68.50	89.37	96.10	69.37	100.00	100.00	100.00	0.0916	46.49	708.00

Table 6: Prediction Evaluation. MAE: Mean Absolute Error, R2: R-squared, NRMSE: Normalized Root Mean Square Error, MET: Mean Evaluation Time, MTT: Mean Training Time.

Approach	Young’s Modulus			Accuracy Shear Modulus			Poisson’s Ratio			Efficiency (ms)	
	MAE \downarrow	$R^2 \uparrow$	NRMSE \downarrow	MAE \downarrow	$R^2 \uparrow$	NRMSE \downarrow	MAE \downarrow	$R^2 \uparrow$	NRMSE \downarrow	MET	MTT
Molecule targeted methods.											
SchNet [58]	0.0005704	0.2304	0.1436	0.0001343	0.01441	0.3958	0.3962	-0.1025	0.02029	3.34	12.39
Spherenet [41]	0.0004744	0.4548	0.1185	0.0001039	0.2839	0.08682	0.3561	-0.01795	0.02499	11.62	33.08
Equiformer [37]	0.0006669	-0.3892	0.2469	0.0002226	-1.1149	0.3459	0.3673	-0.03171	0.05805	63.17	204.70
ViSNet [61]	0.0006223	0.05871	0.1506	0.06375	0.06375	0.1003	0.3699	-0.04497	0.01916	15.63	32.33
Crystal targeted methods.											
CGCNN [63]	0.0006179	0.3550	0.1785	0.0001475	0.09353	0.1720	0.3922	0.04905	0.08282	10.76	48.51
ALIGNN [19]	0.0008320	-1.2955	0.1544	0.0001460	-0.01672	0.09749	0.31267	-0.13298	0.01634	990.34	44993.19
Metamaterial targeted methods.											
uniTruss [69]	0.0006266	0.1812	0.1389	0.0001451	0.06374	0.09955	0.3970	-0.1016	0.02014	1.18	0.22
Mace+ve [26]	0.0003882	0.6692	0.08797	0.0001211	0.1932	0.08913	0.2881	0.1585	0.01738	27.34	304.2

4.2 Algorithms Comparison

Below, we explore how the complex ML models perform on metamaterial applications. We employ our evaluation metrics to compare the integrated algorithms shown in Table 2 regarding both generative and predictive tasks. We train all models on A100 GPUs following each baseline’s original hyperparameters and training strategies. We primarily use the MetaModulus dataset (16,707 samples, split 8,000/2,000/6,707 for train/valid/test) with its three mechanical properties (Young’s modulus, Shear modulus, Poisson’s ratio). Our baselines target molecules, crystals, or metamaterials as shown in Table 2. Methods that cannot handle lattices or edges are adapted accordingly; Large Language Models (LLMs) are pre-trained on crystals and fine-tuned on metamaterials. More implementation details are stated in Appendix D. To comprehensively evaluate these models, we utilize the proposed evaluation toolbox in Table 3 for evaluation. Additional details appear in the Appendix.

Benchmarking Generative Models. Table 5 compares the generation performance of generative models through the evaluation toolbox. In general, we have the following observations: (1) *Periodicity constraints benefit generation:* EDM and GeoLDM (top of Table 5) are molecule-targeted methods. Hence, they do not satisfy crystal-specific constraints (e.g., periodicity) as shown in Table 2. Table 5 suggests that they cannot generate valid and diverse structures. Specifically, it shows up as 0 (or near 0) “validity” on metrics tied to periodicity (\mathcal{V}_P) and symmetry (\mathcal{V}_S), and also 0 coverage (Cov. R

and Cov. P) of test data space. By contrast, crystal-targeted methods (e.g., CDVAE, DiffCSP, EquiCSP, etc.) that generally impose periodicity constraints show higher symmetry and periodicity validities (\mathcal{V}_S and \mathcal{V}_P). We suspect that the molecular-based methods without periodicity constraints cannot adapt to metamaterial generation. (2) *Equivariance tends to boost validity and diversity:* Comparing mean validity of equivariant architectures (EquiCSP and DiffCSP), semi-equivariant architectures (CDVAE and Cond-CDVAE), and invariant architectures (SyMat), the performance decreases accordingly from 29.48% and 20.48% (equivariant), 10.69% and 28.72% (semi-equivariant), to 10.64% (invariant) as per validity; and 96.23% and 76.18% (equivariant), 75.83% and 74.55% (semi-equivariant) to 0.00 (invariant) as per diversity. (3) *LLM approaches excel in all metrics without geometric constraints:* CrystalLLM and Crystal-Text-LLM do not declare explicit geometric constraints (regarding periodicity and symmetry). However, they show superior performance on validity, which may be because the LLMs, despite lacking explicit geometric constraints, can learn valid periodicity and symmetry from a large number of data (both pre-train and finetune data). In addition, their 100% coverage on the test dataset demonstrates their larger design space compared to other methods with geometric constraints. Moreover, their low Conditional Effectiveness indicates adherence to desired conditions during generation. (4) *LLM approaches are training inefficient. More constraints lead to longer generation time.*

Focusing on mean training time per batch (MTT), it can be concluded that the training time of LLM-based methods is many times longer than others. In addition, regarding the generation time per sample (MET), methods with more geometric constraints tend to be less generation efficient.

Benchmarking Predictive Models. We benchmark the predictive models in Table 6, from which we can have the following observations. (1) *Metamaterial oriented methods perform better:* Comparing the three design targets, the metamaterial targeted methods generally perform superior to the other, especially Mace+ve outperforms the second best 0.2144 and 0.1765 regarding R^2 on Young’s modulus and Poisson’s ratio, respectively. uniTruss obtains the best efficiency, although its accuracy is moderate. This superior performance of metamaterial-tailored methods is reasonable since they align well with the dataset. (2) *Periodic constraints are ineffective for accuracy:* Comparing the methods with periodicity constraints (i.e., ViSNet, CGCNN, and ALIGNN), they do not have obvious superiority to the methods without periodicity constraints (e.g., SchNet, SphereNet, Mace+ve, and uniTruss). This observation is different from generation task, and we suspect it is because the mechanical properties is not related to periodicity. (3) *Invariant models are efficient and effective:* Comparing equivariant models (i.e., Equiformer, ViSNet, and Mace+ve) and invariant models (other models), the invariant models demonstrate greater efficiency on both the evaluating and the training phase. Moreover, most invariant models perform better than equivariant models except Mace+ve which is specifically designed for the conducted dataset.

In summary, metamaterial-specific methods (e.g., Mace+ve) perform the best for mechanical property prediction, and LLM-based method is most effective for metamaterial generation. This benchmarking provides guidance on selecting appropriate models for metamaterial research (addressing C2).

4.3 Case Study on Visual-Interactive Interface

Here we provide a case study on how MetamatBench enhances metamaterial design for a specific hypothesis. By integrating the three key modules, the system guides metamaterial researchers from model selection through dataset analytics to predictive simulation, ultimately accelerating the discovery of effective metamaterials. To be specific, in this case study shown in Figure 5, the goal is to design a lattice structure for the fingertip with desired mechanical properties such as Young’s modulus, Shear modulus, and Poisson’s ratio, achieving a balance between stiffness and flexibility. The process begins with **Step 0 (Hypothesis)**, where researchers define the requirement for a fingertip structure that replicates a real hand’s size and mechanics. Moving to **Step 1 (Model and Data Selection)**, they leverage M1 in the visual-interactive interface to identify suitable ML models and datasets. In **Step 2 (Data Analytics)**, the chosen datasets are analyzed to obtain insights into structural-performance relationships, guiding the refinement of the lattice design. Finally, **Step 3 (Human-AI Collaboration)** is where M3 facilitates iterative design: researchers propose modifications based on domain knowledge according to their analysis of Step 2, while the AI predicts the fingertip’s mechanical responses and generate specific lattice structures, leading to rapid refinements of both the hypothesis and the metamaterial structure. As a result,

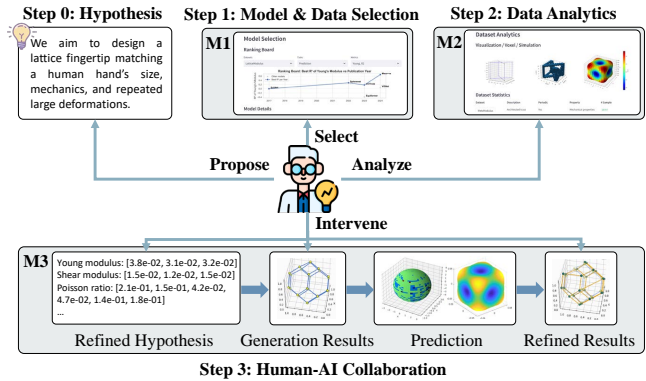


Figure 5: A case study on human-AI collaboration for metamaterial discovery.

users found the visualizations of refined results intuitive. This loop of expert feedback and AI-driven prediction expedites the development of a lattice fingertip optimized for finger-like mechanical performance.

5 Conclusion and Future Work

In this paper, we propose a multi-level system, MetamatBench, to bridge the gap between traditional metamaterial research and advanced ML methodologies. At the data level, our unified data processing and representation framework addresses the inherent data heterogeneity in metamaterial datasets. The intermediate ML level handles model complexity by offering an extensive ML toolbox—comprising both a model suite and a multi-perspective evaluation toolkit—while the top level addresses dual black-box challenge between human and the AI system through a visual-interactive visual-interactive interface that reduces the opacity of human-AI collaboration. Our experimental results demonstrate enhanced data validity, provide an in-depth analysis of ML model performance in metamaterial contexts, and illustrate the system’s potential to accelerate metamaterial discoveries with a case study.

Looking forward, we propose two research directions to advance both ML and metamaterials. **Q1:** Design ML models that integrate geometric constraints unique to metamaterials. **Q2:** Strengthen collaborations between metamaterial researchers and AI systems to drive innovative breakthroughs.

Acknowledgments

We thank the anonymous reviewers for their constructive comments. This work is supported by the National Science Foundation under Award No. IIS-2339989 and No. 2406439, DARPA under contract No. HR00112490370 and No. HR001124S0013, U.S. Department of Homeland Security under Grant Award No. 17STCIN00001-08-00, Amazon-Virginia Tech Initiative for Efficient and Robust Machine Learning, Amazon AWS, Google, Cisco, 4-VA, Commonwealth Cyber Initiative, National Surface Transportation Safety Center for Excellence, and Virginia Tech. The views and conclusions are those of the authors and should not be interpreted as representing the official policies of the funding agencies or the government.

References

- [1] 2019. A 149 line homogenization code for three-dimensional cellular materials written in MATLAB. *Journal of Engineering Materials and Technology* 141, 1 (Jan. 2019). doi:10.1115/1.4040555
- [2] Erik Andreassen and Casper Schousboe Andreassen. 2014. How to determine composite material properties using numerical homogenization. *Computational Materials Science* 83 (2014), 488–495. doi:10.1016/j.commatsci.2013.09.006
- [3] Anonymous. 2025. UniMate: A Unified Model for Mechanical Metamaterial Generation, Property Prediction, and Condition Confirmation. In *Forty-second ICML*. <https://openreview.net/forum?id=X7uVxeFS9A>
- [4] Luis M Antunes, Keith T Butler, and Ricardo Grau-Crespo. 2024. Crystal structure generation with autoregressive large language modeling. *Nature Communications* 15, 1 (2024), 1–16.
- [5] Sajad Arabnejad and Damiano Pasini. 2013. Mechanical properties of lattice materials via asymptotic homogenization and comparison with alternative homogenization methods. *International Journal of Mechanical Sciences* 77 (2013), 249–262. doi:10.1016/j.ijmecsci.2013.10.003
- [6] Kenneth Atz, Francesca Grisoni, and Gisbert Schneider. 2021. Geometric deep learning on molecular representations. *Nature Machine Intelligence* 3, 12 (2021), 1023–1032.
- [7] Luis Barroso-Luque, Muhammed Shuaibi, Xiang Fu, Brandon M. Wood, Misko Dzamba, Meng Gao, Ammar Rizvi, C. Lawrence Zitnick, and Zachary W. Ulissi. 2024. Open Materials 2024 (OMat24) Inorganic Materials Dataset and Models. arXiv:2410.12771 <https://arxiv.org/abs/2410.12771>
- [8] Jan-Hendrik Bastek and Dennis M Kochmann. 2023. Inverse design of nonlinear mechanical metamaterials via video denoising diffusion models. *Nature Machine Intelligence* 5, 12 (2023), 1466–1475.
- [9] Jan-Hendrik Bastek, Siddhant Kumar, Bastian Telgen, Raphaël N Glaesener, and Dennis M Kochmann. 2022. Inverting the structure–property map of truss metamaterials by deep learning. *Proceedings of the National Academy of Sciences* 119, 1 (2022), e2111505119.
- [10] Ilyes Batatia, David Peter Kovacs, Gregor N. C. Simm, Christoph Ortner, and Gabor Csanyi. 2022. MACE: Higher Order Equivariant Message Passing Neural Networks for Fast and Accurate Force Fields. In *NeurIPS*, Alice H. Oh, Alekh Agarwal, Danielle Belgrave, and Kyunghyun Cho (Eds.).
- [11] Simon Batzner, Albert Musaelian, Lixin Sun, Mario Geiger, Jonathan P Mailoa, Mordechai Korbbluth, Nicola Molinari, Tess E Smidt, and Boris Kozinsky. 2022. E (3)-equivariant graph neural networks for data-efficient and accurate interatomic potentials. *Nature communications* 13, 1 (2022), 2453.
- [12] Stanislav S Borysov, R Matthias Geilhufer, and Alexander V Balatsky. 2017. Organic materials database: An open-access online database for data mining. *PLoS one* 12, 2 (2017), e0171501.
- [13] Ivano E Castelli, David D Landis, Kristian S Thygesen, Søren Dahl, Ib Chorkendorff, Thomas F Jaramillo, and Karsten W Jacobsen. 2012. New cubic perovskites for one- and two-photon water splitting using the computational materials repository. *Energy & Environmental Science* 5, 10 (2012), 9034–9043.
- [14] Ivano E Castelli, Thomas Olsen, Soumendu Datta, David D Landis, Søren Dahl, Kristian S Thygesen, and Karsten W Jacobsen. 2012. Computational screening of perovskite metal oxides for optimal solar light capture. *Energy & Environmental Science* 5, 2 (2012), 5814–5819.
- [15] Yu-Chin Chan, Faez Ahmed, Liwei Wang, and Wei Chen. 2021. METASET: Exploring shape and property spaces for data-driven metamaterials design. *Journal of Mechanical Design* 143, 3 (2021), 031707.
- [16] Lowik Chanussot, Abhishek Das, Siddharth Goyal, Thibaut Lavril, Muhammed Shuaibi, Morgane Riviere, Kevin Tran, Javier Heras-Domingo, Caleb Ho, Weihua Hu, et al. 2021. Open catalyst 2020 (OC20) dataset and community challenges. *Acs Catalysis* 11, 10 (2021), 6059–6072.
- [17] Jianpeng Chen, Yawen Ling, Jie Xu, Yazhou Ren, Shudong Huang, Xiaorong Pu, Zhifeng Hao, Philip S. Yu, and Lifang He. 2025. Variational Graph Generator for Multiview Graph Clustering. *IEEE TNLS* (2025), 1–14. doi:10.1109/TNLS.2024.3524205
- [18] Tingwei Chen, Jianpeng Chen, and Dawei Zhou. 2024. 3D-FuM: benchmarking 3D molecule learning with functional groups. In *Proceedings of the Thirty-Third IJCAI*. 8635–8639.
- [19] Kamal Choudhary and Brian DeCost. 2021. Atomistic line graph neural network for improved materials property predictions. *npj Computational Materials* 7, 1 (2021), 185.
- [20] Yuanqi Du, Yingheng Wang, Yining Huang, Jianan Canal Li, Yanqiao Zhu, Tian Xie, Chenru Duan, John Gregoire, and Carla P Gomes. 2023. M² Hub: Unlocking the Potential of Machine Learning for Materials Discovery. *NeurIPS* 36 (2023), 77359–77378.
- [21] Alexander Dunn, Qi Wang, Alex Ganose, Daniel Dopp, and Anubhav Jain. 2020. Benchmarking materials property prediction methods: the Matbench test set and Automattminer reference algorithm. *npj Computational Materials* 6, 1 (2020), 138.
- [22] Nader Engheta and Richard W Ziolkowski. 2006. *Metamaterials: physics and engineering explorations*. John Wiley & Sons.
- [23] Evan N Feinberg, Debnil Sur, Zhenqin Wu, Brooke E Husic, Huanghao Mai, Yang Li, Saisai Sun, Jianyi Yang, Bharath Ramsundar, and Vijay S Pande. 2018. PotentialNet for molecular property prediction. *ACS central science* 4, 11 (2018), 1520–1530.
- [24] Octavian Ganea, Lagnajit Pattanaik, Connor Coley, Regina Barzilay, Klavs Jensen, William Green, and Tommi Jaakkola. 2021. GeoMol: Torsional Geometric Generation of Molecular 3D Conformer Ensembles. In *NeurIPS*, M. Ranzato, A. Beygelzimer, Y. Dauphin, P.S. Liang, and J. Wortman Vaughan (Eds.), Vol. 34. Curran Associates, Inc., 13757–13769. https://proceedings.neurips.cc/paper_files/paper/2021/file/725215ed82ab6306919b485b81ff9615-Paper.pdf
- [25] Johannes Gasteiger, Florian Becker, and Stephan Günnemann. 2021. Gemnet: Universal directional graph neural networks for molecules. *NeurIPS* 34 (2021), 6790–6802.
- [26] Ivan Grega, Ilyes Batatia, Gabor Csanyi, Sri Karlapati, and Vikram Deshpande. 2024. Energy-conserving equivariant GNN for elasticity of lattice architected metamaterials. In *ICLR*.
- [27] Nate Gruver, Anuroop Sriram, Andrea Madotto, Andrew Gordon Wilson, C. Lawrence Zitnick, and Zachary Ward Ulissi. 2024. Fine-Tuned Language Models Generate Stable Inorganic Materials as Text. In *The Twelfth ICLR*. <https://openreview.net/forum?id=vN9pfqoP1>
- [28] Emiel Hoogeboom, Victor Garcia Satorras, Clément Vignac, and Max Welling. 2022. Equivariant diffusion for molecule generation in 3d. In *ICML*. PMLR, 8867–8887.
- [29] Padmeya Prashant Indurkar, Sri Karlapati, Angkur Jyoti Dipanka Shaikkea, and Vikram S Deshpande. 2022. Predicting deformation mechanisms in architected metamaterials using GNN. *arXiv preprint arXiv:2202.09427* (2022).
- [30] Anubhav Jain, Shyue Ping Ong, Geoffroy Hautier, Wei Chen, William Davidson Richards, Stephen Dacek, Shreyas Cholia, Dan Gunter, David Skinner, Gerbrand Ceder, et al. 2013. Commentary: The Materials Project: A materials genome approach to accelerating materials innovation. *APL materials* 1, 1 (2013).
- [31] Zian Jia, Fan Liu, Xihang Jiang, and Lifeng Wang. 2020. Engineering lattice metamaterials for extreme property, programmability, and multifunctionality. *Journal of Applied Physics* 127, 15 (2020).
- [32] Rui Jiao, Wenbing Huang, Peijia Lin, Jiaqi Han, Pin Chen, Yutong Lu, and Yang Liu. 2023. Crystal Structure Prediction by Joint Equivariant Diffusion on Lattices and Fractional Coordinates. In *Workshop on "Machine Learning for Materials" ICLR 2023*. <https://openreview.net/forum?id=VPByphdu24j>
- [33] John Jumper, Richard Evans, Alexander Pritzel, Tim Green, Michael Figurnov, Olaf Ronneberger, Kathryn Tunyasuvunakool, Russ Bates, Augustin Židek, Anna Potapenko, et al. 2021. Highly accurate protein structure prediction with AlphaFold. *nature* 596, 7873 (2021), 583–589.
- [34] Nicolas Keriven and Gabriel Peyré. 2019. Universal invariant and equivariant graph neural networks. *NeurIPS* 32 (2019).
- [35] Thomas N Kipf and Max Welling. 2016. Semi-supervised classification with graph convolutional networks. *arXiv preprint arXiv:1609.02907* (2016).
- [36] Thomas N Kipf and Max Welling. 2016. Variational graph auto-encoders. *arXiv preprint arXiv:1611.07308* (2016).
- [37] Yi-Lun Liao and Tess Smidt. 2023. Equiformer: Equivariant Graph Attention Transformer for 3D Atomistic Graphs. In *The Eleventh ICLR*. <https://openreview.net/forum?id=KwmPfaRgOTD>
- [38] Yi-Lun Liao, Brandon M Wood, Abhishek Das, and Tess Smidt. 2024. EquiformerV2: Improved Equivariant Transformer for Scaling to Higher-Degree Representations. In *The Twelfth ICLR*. <https://openreview.net/forum?id=mCOBKZmrzD>
- [39] Peijia Lin, Pin Chen, Rui Jiao, Qing Mo, Cen Jianhuan, Wenbing Huang, Yang Liu, Dan Huang, and Yutong Lu. 2024. Equivariant Diffusion for Crystal Structure Prediction. In *Forty-first ICML*.
- [40] Shengchao Liu, Yanjing Li, Zhuoxinran Li, Zhiling Zheng, Chenru Duan, Zhi-Ming Ma, Omar Yaghi, Animashree Anandkumar, Christian Borgs, Jennifer Chayes, et al. 2024. Symmetry-informed geometric representation for molecules, proteins, and crystalline materials. *NeurIPS* 36 (2024).
- [41] Yi Liu, Limei Wang, Meng Liu, Yuchao Lin, Xuan Zhang, Bora Oztekin, and Shuiwang Ji. 2022. Spherical Message Passing for 3D Molecular Graphs. In *ICLR*.
- [42] Thomas S Lumpe and Tino Stankovic. 2021. Exploring the property space of periodic cellular structures based on crystal networks. *Proceedings of the National Academy of Sciences* 118, 7 (2021), e2003504118.
- [43] Xiaoshan Luo, Zhenyu Wang, Pengyue Gao, Jian Lv, Yanchao Wang, Changfeng Chen, and Yanming Ma. 2024. Deep learning generative model for crystal structure prediction. *npj Computational Materials* 10, 1 (2024), 254.
- [44] Youzhi Luo, Chengkai Liu, and Shuiwang Ji. 2024. Towards Symmetry-Aware Generation of Periodic Materials. *NeurIPS* 36 (2024).
- [45] Youzhi Luo, Chengkai Liu, and Shuiwang Ji. 2024. Towards symmetry-aware generation of periodic materials. *NeurIPS* 36 (2024).
- [46] Paul P Meyer, Colin Bonatti, Thomas Tancogne-Dejean, and Dirk Mohr. 2022. Graph-based metamaterials: Deep learning of structure-property relations. *Materials & Design* 223 (2022), 111175.
- [47] R Otto, J Brox, S Trippel, M Stei, T Best, and R Wester. 2012. Single solvent molecules can affect the dynamics of substitution reactions. *Nature chemistry* 4, 7 (2012), 534–538.

- [48] Emin Emre Ozdilek, Egecan Ozcakar, Nitel Muhtaroglu, Ugur Simsek, Orhan Gulcan, and Gullu Kiziltas Sendur. 2024. A finite element based homogenization code in python: HomPy. *Advances in Engineering Software* 194 (2024), 103674. doi:10.1016/j.advengsoft.2024.103674
- [49] Michael O'keeffe, Maxim A Peskov, Stuart J Ramsden, and Omar M Yaghi. 2008. The reticular chemistry structure resource (RCSR) database of, and symbols for, crystal nets. *Accounts of chemical research* 41, 12 (2008), 1782–1789.
- [50] Dilip D Paul. 2010. Optical metamaterials: fundamentals and applications.
- [51] Chris J Pickard. 2020. AIRSS data for carbon at 10GPa and the C+ N+ H+ O system at 1GPa. (*No Title*) (2020).
- [52] Jingyuan Qi, Zian Jia, Minqian Liu, Wangzhi Zhan, Junkai Zhang, Xiaofei Wen, Jingru Gan, Jianpeng Chen, Qin Liu, Mingyu Derek Ma, Bangzheng Li, Haohui Wang, Adithya Kulkarni, Muhao Chen, Dawei Zhou, Ling Li, Wei Wang, and Lifu Huang. 2025. MetaScientist: A Human-AI Synergistic Framework for Automated Mechanical Metamaterial Design. In *Proceedings of the 2025 Conference of the Nations of the Americas Chapter of the Association for Computational Linguistics (NAACL): Human Language Technologies (System Demonstrations)*. Association for Computational Linguistics, Albuquerque, New Mexico, 404–436. <https://aclanthology.org/2025.naacl-demo.34/>
- [53] Raghunathan Ramakrishnan, Pavlo O Dral, Matthias Rupp, and O Anatole Von Lilienfeld. 2014. Quantum chemistry structures and properties of 134 kilo molecules. *Scientific data* 1, 1 (2014), 1–7.
- [54] SJ Ramsden, Vanessa Robins, and ST Hyde. 2009. Three-dimensional Euclidean nets from two-dimensional hyperbolic tilings: kaleidoscopic examples. *Acta Crystallographica Section A: Foundations of Crystallography* 65, 2 (2009), 81–108.
- [55] Andrew S Rosen, Victor Fung, Patrick Huck, Cody T O'Donnell, Matthew K Horton, Donald G Truhlar, Kristin A Persson, Justin M Notestein, and Randall Q Snurr. 2022. High-throughput predictions of metal–organic framework electronic properties: theoretical challenges, graph neural networks, and data exploration. *npj Computational Materials* 8, 1 (2022), 1–10.
- [56] Victor Garcia Satorras, Emiel Hoogeboom, and Max Welling. 2021. E (n) equivariant graph neural networks. In *ICML*. PMLR, 9323–9332.
- [57] Victor Garcia Satorras, Emiel Hoogeboom, and Max Welling. 2021. E(n) Equivariant Graph Neural Networks. In *ICML*. 9323–9332.
- [58] Kristof Schütt, Pieter-Jan Kindermans, Huziel EnoC Saucedo Felix, Stefan Chmiela, Alexandre Tkatchenko, and Klaus-Robert Müller. 2017. SchNet: A continuous-filter convolutional neural network for modeling quantum interactions. *NeurIPS* 30 (2017).
- [59] Haohui Wang, Weijie Guan, Jianpeng Chen, Zi Wang, and Dawei Zhou. 2024. Towards Heterogeneous Long-tailed Learning: Benchmarking, Metrics, and Toolbox. In *NeurIPS Datasets and Benchmarks Track*.
- [60] Tong Wang, Xinheng He, Mingyu Li, Yatao Li, Ran Bi, Yusong Wang, Chaoran Cheng, Xiangzhen Shen, Jiawei Meng, He Zhang, et al. 2024. Ab initio characterization of protein molecular dynamics with AI2BMD. *Nature* (2024), 1–9.
- [61] Yusong Wang, Tong Wang, Shaoning Li, Xinheng He, Mingyu Li, Zun Wang, Nanning Zheng, Bin Shao, and Tie-Yan Liu. 2024. Enhancing geometric representations for molecules with equivariant vector-scalar interactive message passing. *Nature Communications* 15, 1 (2024), 313.
- [62] Tian Xie, Xiang Fu, Octavian-Eugen Ganea, Regina Barzilay, and Tommi S Jaakkola. 2022. Crystal Diffusion Variational Autoencoder for Periodic Material Generation. In *ICLR*. https://openreview.net/forum?id=03RLpj-tc_
- [63] Tian Xie and Jeffrey C Grossman. 2018. Crystal graph convolutional neural networks for an accurate and interpretable prediction of material properties. *Physical review letters* 120, 14 (2018), 145301.
- [64] Minkai Xu, Shitong Luo, Yoshua Bengio, Jian Peng, and Jian Tang. 2021. Learning Neural Generative Dynamics for Molecular Conformation Generation. In *ICLR*. <https://openreview.net/forum?id=pAbm1qfheGk>
- [65] Minkai Xu, Alexander S Powers, Ron O. Dror, Stefano Ermon, and Jure Leskovec. 2023. Geometric Latent Diffusion Models for 3D Molecule Generation. In *Proceedings of the 40th ICML*, Vol. 202. 38592–38610.
- [66] Qiaofeng Yao, Xun Yuan, Tiankai Chen, David Tai Leong, and Jianping Xie. 2018. Engineering functional metal materials at the atomic level. *Advanced Materials* 30, 47 (2018), 1802751.
- [67] Claudio Zeni, Robert Pinsler, Daniel Zügner, Andrew Fowler, Matthew Horton, Xiang Fu, Zilong Wang, Aliaksandra Shysheya, Jonathan Crabbé, Shoko Ueda, et al. 2025. A generative model for inorganic materials design. *Nature* (2025), 1–3.
- [68] Li Zheng, Konstantinos Karapiperis, Siddhant Kumar, and Dennis M Kochmann. 2023. Unifying the design space and optimizing linear and nonlinear truss metamaterials by generative modeling. *Nature Communications* 14, 1 (2023), 7563.
- [69] Li Zheng, Konstantinos Karapiperis, Siddhant Kumar, and Dennis M Kochmann. 2023. Unifying the design space and optimizing linear and nonlinear truss metamaterials by generative modeling. *Nature Communications* 14, 1 (2023), 7563.
- [70] Nils ER Zimmermann and Anubhav Jain. 2020. Local structure order parameters and site fingerprints for quantification of coordination environment and crystal structure similarity. *RSC advances* 10, 10 (2020), 6063–6081.